Food Research International 178 (2024) 114008

Contents lists available at ScienceDirect

Food Research International

journal homepage: www.elsevier.com/locate/foodres

Mass spectrometry-based quantification of immunostimulatory gliadin proteins and peptides in coloured wheat varieties: Implications for Celiac Disease

Ricardo Dias [a,*], Sara da Silva [a], Bruna Monteiro [a], Rosa Pérez-Gregorio [a,b], Nuno Mateus [a], Carmen Gianfrani [c], Maria Vittoria Barone [d], Petr Martinek [e], Victor Freitas [a]

[a] LAQV-REQUIMTE, Department of Chemistry and Biochemistry, Faculty of Sciences of the University of Porto, Porto, Portugal
[b] Department of Analytical and Food Chemistry. Nutrition and Bromatology Area. Faculty of Sciences of the University of Vigo, Ourense, Spain
[c] Institute of Biochemistry and Cell Biology, Department of Biomedical Sciences, National Research Council of Italy, Naples, Italy
[d] ELFID (European Laboratory for the Investigation of Food Induced Diseases), Department of Translational Medical Science, Section of Paediatrics, University Federico II, Naples, Italy
[e] Agrotest Fyto, Ltd., Kroměřříž, Czech Republic

ARTICLE INFO

Keywords:
Pigmented wheat
Gluten
Protein expression profiling
Data-dependent acquisition

ABSTRACT

Pigmented wheat varieties (*Triticum aestivum* spp.) are getting increasingly popular in modern nutrition and thoroughly researched for their functional and nutraceutical value. The colour of these wheat grains is caused by the expression of natural pigments, including carotenoids and anthocyanins, that can be restricted to either the endosperm, pericarp and/or aleurone layers. While contrasts in phytochemical synthesis give rise to variations among purple, blue, dark and yellow grain's antioxidant and radical scavenging capacities, little is known about their influence on gluten proteins expression, digestibility and immunogenic potential in a Celiac Disease (CD) framework. Herein, it has been found that the expression profile and immunogenic properties of gliadin proteins in pigmented wheat grains might be affected by anthocyanins and carotenoids upregulation, and that the spectra of peptide released upon simulated gastrointestinal digestion is also significantly different. Interestingly, anthocyanin accumulation, as opposed to carotenoids, correlated with a lower immunogenicity and toxicity of gliadins at both protein and peptide levels. Altogether, this study provides first-level evidence on the impact modern breeding practices, seeking higher expression levels of health promoting phytochemicals at the grain level, may have on wheat crops functionality and CD tolerability.

1. Introduction

Wheat, the world's most widely cultivated cereal, has served as a vital food source for over 10,000 years due to its rich content of macronutrients, including carbohydrates, proteins, and fiber, as well as essential micronutrients like vitamins and minerals (Erenstein et al., 2022). Consuming wheat in its whole grain form is associated with health benefits such as reducing the risk of type 2 diabetes, cardiovascular diseases, and cancer mortality (Reynolds, Akerman, & Mann, 2020; Zhang, Zhao, Guo, Bao, & Wang, 2018). However, the milling process, which removes the germ and bran from the grain to achieve desired flour properties, often strips away many of these valuable nutrients (Awika, 2011; Cappelli & Cini, 2021). The challenge thus lies in developing wheat-based products that maintain their texture and flavour while preserving the health benefits of unprocessed wheat.

Consumers today prioritize health and seek new, natural food sources with functional benefits, including naturally coloured foods that offer improved nutrition and antioxidants (Saini et al., 2021). Coloured wheat varieties have gained attention for their potential benefits, and it's crucial to explore how these varieties outperform common wheat in terms of nutritional value and applications in whole wheat flours. Common flour is typically derived from red or white wheat grains, resulting in an amber-coloured product. In contrast, coloured wheat species, rich in phytochemicals like anthocyanins, flavonoids, carotenoids, and other phenolic compounds, not only provide vibrant colours to the grains but also offer enhanced antioxidant properties and potential

* Corresponding author.
E-mail address: ricardo.dias@fc.up.pt (R. Dias).

https://doi.org/10.1016/j.foodres.2024.114008
Received 13 November 2023; Received in revised form 5 January 2024; Accepted 9 January 2024
Available online 11 January 2024
0963-9969/© 2024 The Author(s). Published by Elsevier Ltd. This is an open access article under the CC BY license (http://creativecommons.org/licenses/by/4.0/).

Table 1
Description of wheat (*Triticum aestivum L.*) genotypes. CZE – Czech Republic, SVK – Slovakia.

Cultivar	Growth type	Country of origin	Cultivar status	Pedigree	Grain color
Bohemia	Winter	CZE	Released	(540i-92 × 6192a-92) × (540i-92 × Kontrast)	Red
Bona Vita	Winter	SVK	Released	(SO-690 × Arida) × Arida	Yellow endosperm
AF Jumiko	Winter	CZE	Released (2018)	ANK-28A × Meritto	Purple pericarp
AF Oxana	Winter	CZE	Released (2019)	RU 440–6 × Ludwig	Blue aleurone
AF Zora	Winter	CZE	Released (2021)	(Skorpion × Bohemia) × (Indigo x Bohemia)	Black

health benefits. Different varieties of coloured wheat can feature higher carotenoid content in the endosperm, such as yellow wheat, or greater anthocyanin content in various external kernel layers, including pericarps for purple wheat, aleurone layers for blue wheat, and both layers for black wheat (Garg et al., 2022; Paznocht, Burešová, Kotíková, & Martinek, 2021).

Yellow endosperm wheat varieties are characterized by their high carotenoid content, particularly lutein and zeaxanthin, along with other carotenoids in smaller amounts. In contrast, purple, blue, and black wheat varieties exhibit a broader range of phenolic compounds, including anthocyanins, flavonoids, and other polyphenols. The primary distinction among these coloured wheat types lies in the dominant anthocyanins they contain, such as cyanidin-3-glucoside in purple wheat, delphinidin derivatives in blue wheat, and variable concentrations of cyanidin and delphinidin derivatives in black wheat (Abdel-Aal et al., 2008; Abdel-Aal, Hucl, Shipp, & Rabalski, 2016; Ficco et al., 2014; Lachman, Martinek, Kotíková, Orsák, & Šulc, 2017). The anthocyanin content in pigmented wheat grains, however, depends on several variables including environmental factors (*e.g.* climate, soil type, sunlight exposure, and mycotoxin infection), agricultural practices (*e.g.* nitrogen fertilization) and technological processes (Gozzi et al., 2023; Sardella et al., 2023).

Apart from other non-communicable disease conditions, coloured wheat grains also hold potential for use in wheat-related diseases like Celiac Disease (CD), thanks to their antioxidant properties that could mitigate damage caused by gluten consumption (Dias, Pereira, Pérez-Gregorio, Mateus, & Freitas, 2021; Ribeiro, Sousa, Poeta, Bagulho, & Igrejas, 2020). However, current studies primarily focus on genetic differences and phenolic content, which provide the desired antioxidant properties, rather than the gluten and gliadin protein composition (the main triggers of CD). Assessing the gluten content of these coloured wheat flours is essential to determine their suitability in CD management – when compared to traditional wheat flours -, considering the varying immunoreactive responses triggered by different gliadin peptides in CD patients. In line with such need, this study intends to provide (1) an in-depth qualitative and quantitative profiling of gliadin proteins and peptides from pigmented wheat grains by bottom-up proteomics, and (2) investigate the changes in gliadin digestibility and immunogenicity in relation to the upregulation of anthocyanins and carotenoids.

2. Material and methods

2.1. Reagents

The quality of all chemicals was of analytical grade, unless stated otherwise. P31–43 (*seq.* LGQQQPFPPQQPY, purity ≥98 %) and p58–89 (*seq.* QLQPFPQPQLPYPQPQLPYPQPQLPYPQPQPF, purity ≥98 %) were both purchased to GenScript (Rijswijk, Netherlands).

2.2. Plant materials

A total of five coloured-grain wheat genotypes were grown in 2019/2020 at the *Agricultural Research Institute* in Kroměříž, Czech Republic (49.2851172N, 17.3646269E). The experimental field is located 235 m above sea level, has Luvic Chernozem (Loamic) soil, an average annual temperature 9.2 °C, mild winters, and annual precipitation averaging 576 mm. The plants were grown on experimental plots (10 m^2) using conventional growing technologies. Each wheat genotype was grown on 5 independent plots, which were harvested separately and 1 kg of grain from each experimental plot was used to create a sample. Until further processing, grains were stored in cloth bags (in the dark) at a temperature of 22 °C. The main characteristics of the selected wheat genotypes are listed in Table 1.

2.3. Wholemeal flour milling

Before milling, grains were cleaned by sieving them through a 2 mm sieve, and the remaining impurities manually removed. Wholemeal flours were prepared on an Ultra Centrifugal Mill ZM 200, with a rotor speed of 15.000 rpm and screen aperture size of 250 μm (*Retsch Inc., Germany*). Flours were immediately cooled to −20 °C and kept at this temperature until analysis to protect bioactive components from degradation. For comparison purposes, a commercial Portuguese type 65 wheat flour (*from Espiga, Fábricas Lusitana Produtos Alimentares, SA*) was used as an example of an industrially processed wheat grain.

2.4. Extraction of gliadin proteins

The extraction of proline and glutamine-rich gliadin proteins from petroleum-ether defatted flours was carried out in accordance with previous methods (da Silva, Pérez-Gregorio, Mateus, Freitas, & Dias, 2023). Initially, 10 g of type 65 wheat flour underwent defatting twice with diethyl ether (50 mL) for a duration of 30 min. Subsequently, albumin and globulin proteins were extracted through a three-step process involving the resuspension of the defatted flour in a 0.4 mol/L NaCl, 0.067 mol/L NaH_2PO_4 buffer with a pH of 7.5 (50 mL). The suspensions were agitated at room temperature (RT) for 10 min and then subjected to centrifugation at 15,000*g* for 15 min. The subsequent extraction of gliadins from the pellet was accomplished by introducing a water/ethanol mixture (50 mL) to achieve a final ethanol concentration of 70 % (v/v). This mixture was shaken for 45 min at RT and then centrifuged at 15,000*g* for 10 min. The resulting pellets were subjected to two additional extraction cycles using the same outlined procedure. During the transition from albumin/globulin extraction to gliadin extraction, the pellet was rinsed twice with ultrapure water. After completing the extraction steps, the ethanol was eliminated using a rotary evaporator set at 37 °C. The resulting supernatants were subjected to freeze-drying and subsequently stored at −20 °C. The extraction procedure was repeated three times, and the gliadins pooled.

2.5. Reversed-phase high-performance liquid chromatography (RP-HPLC)

Resolubilized and filtered (13 mm/0.45 μm RC) aqueous gliadin solutions, at 1 mg/mL, were analysed by RP-HPLC on a Dionex UltiMate 3000 RSLC system (*Thermo Fisher Scientific*, USA) attaching an Acclaim™ 300 C18 HPLC column (particle size 3 μm, 2.1 × 150 mm) at 60 °C. Detection was carried out at 214 and 280 nm using a diode array detector (Dionex Ultimate 3000 Diode Array Detector). Solvents were (A) water/TFA (99.9:0.1; v/v) and (B) acetonitrile/TFA (99.9:0.1; v/v)

Table 2
Marker peptide transitions and detection window parameters for quantitative parallel reaction monitoring mass spectrometry. Amino acid sequence denoted in one letter code.

Peptide name	Peptide sequence	Molecular weight (Da)	Precursor (*m/z*)	Quantifier fragment ions (*m/z*)
p31–43	LGQQQPFPPQQPY	1,527.68	980.4991 (+2)	279.1341 (y_2)
p58–89	qLQPFPQPQLPYPQPQLPYPQPQLPYPQPQPF	3,798.36	1,266.9917 (+2)	263.1385 (y_2)824.4287 (b_{21})

with the gradient 20–60 % B over 60 min, at a flow rate of 0.2 mL/min. The sample injection volume was 20 μL. After each run the column was cleaned with 90 % B for 10 min and equilibrated with the starting solvent for 15 min. Data processing and peak integration was performed using the Chromeleon™ Chromatography Data System (CDS) Software from *Thermo Scientific*.

2.6. Data acquisition for label-free quantification (LFQ) of gluten proteins

The protein composition and abundance within each gliadin sample was assessed through untargeted LC-MS/MS analysis. Initially, gliadins were dissolved in a solution comprising 50 mmol/L Tris-HCl, 8 mol/L urea, adjusted to pH 8, resulting in a final concentration of 5 mg/mL. To prepare the gliadin samples for analysis, 100 μL of each solution were aliquoted into 1.0 mL microcentrifuge tubes. Then, 4 μL of 500 mmol/L DTT was added to each tube to a final concentration of 20 mmol/L. Subsequently, the mixtures were subjected to a heat treatment at 95 °C for 10 min and left to cool at room temperature. For protein alkylation, 4 μL of 1 mol/L iodoacetamide was introduced into each tube, followed by an incubation period in darkness lasting 30 min. The alkylation reaction was then quenched by adding 500 mmol/L DTT solution to a final concentration of 10 mM (1:50 dilution). This step was followed by the addition of MS-grade, Pierce™ Trypsin Protease solution to each sample (previously diluted 10 times with 50 mmol/L Tris-HCl, 1 mmol/L $CaCl_2$, pH 8) to a final protease to protein ratio of 1:25 (w/w). The reactions were allowed to stir overnight at 37 °C at 300 rpm. To prepare for MS analysis, the peptide samples (10 μg) were desalted and concentrated using C18 GL-Tips SDB (*GL Sciences Inc.*, Japan), following the manufacturer's guidelines. Subsequently, the prepared samples (2 μg) were introduced into a Dionex UltiMate 3000 RSLCnano system (*Thermo Fisher Scientific*, USA) coupled to an Orbitrap Q-Exactive™ HF mass spectrometer through an EASY-nano spray source (*Thermo Fisher Scientific*, USA). The peptides were separated using a PepMap C18 column (2 μm, 75 cm × 150 μm) and solvents consisting of water/formic acid (99.8:0.2, v/v) (A) and acetonitrile/formic acid (99.8:0.2, v/v) (B). The separation was performed at a flow rate of 0.200 μL/min, with an injection volume of 10 μL, employing a linear gradient: 0–3 min 10 % B, 90 min 55 % B, 110 min 95 % B, 125 min 95 % B, 130–145 min 10 % B. The ESI interface operated under the following parameters: positive mode, capillary voltage set to 9 V, capillary temperature at 275.0 °C, tube lens set to 100 V, and a spray voltage of 1.9 kV. The MS instrument settings were configured as follows: full scan resolution set to 120,000, AGC target of 3×10^6, *m/z* range spanning from 300 to 2,000, and a maximum injection time 200 ms, The MS/MS settings were adjusted to a resolution of 30,000, helium as the collision gas, normalized collision energy set at 30 %, AGC target of 1×10^5, maximum injection time of 150 ms and an isolation width (*m/z*) of 3.0. All MS and MS/MS spectra were acquired using a data-dependent positive mode, wherein the instrument executed one MS scan followed by an MS/MS scan of the 15 most intense peaks with a minimum AGC target of 7×10^3 and an intensity threshold of 7×10^4. Dynamic exclusion parameters included an exclusion duration of 30.0 s. Charge states of 1, as well as unassigned ones, were excluded from consideration. For internal mass calibration, the following *m/z* signals were used as lock masses: 371.10124, 519.13882, 610.18416.

2.7. Static in vitro simulation of gastrointestinal gliadin digestion

The experiment involving the digestion of gliadin proteins in vitro followed a recently established protocol as outlined in Brodkorb et *al.*'s work from 2019 (Brodkorb et al., 2019). To summarize, 0.2 g of protein were dissolved in 1.4 mL of simulated salivary fluid (containing 75 U/mL of salivary alpha-amylase) and incubated at 37 ℃ for 2 min. Subsequently, 3 mL of simulated gastric juice (pH 3.0) containing pepsin (2000 U/mL of digesta) were introduced, and the mixture was incubated at 37 ℃ for 120 min. Following this, 6 mL of simulated intestinal fluid (pH 7.0), which included 100 U/mL of pancreatin and 10 mmol/L bile, were added, and the incubation continued for another 120 min at 37 ℃. Throughout the entire digestion process, constant mixing was ensured by placing the samples on a rotating wheel. The digestion was halted by heating the samples to 95 ℃ for 5 min. Afterward, the resulting peptide mixtures underwent solid-phase extraction (for desalting) using 35 cc Oasis HLB cartridges from Waters, following the manufacturer's instructions. These cartridges were first prepared by conditioning them with methanol and equilibrating them with ultrapure water. Once the peptide mixtures were loaded, the cartridges were washed with 50 to 100 mL of water, and the peptides were eluted using a solution of methanol and acetonitrile (50:50, v/v) with a volume of 250 mL. The organic solvent was then removed from the eluate using a rotatory evaporator at 37 ℃. The resulting material was reconstituted in ultrapure water and subjected to freeze-drying. The identification of proteolytically-resistant gluten peptides was carried out using mass spectrometry, employing the same chromatographic and MS/MS parameters as previously described.

2.8. Targeted MS analyses

LFQ of two immunostimulatory gluten peptides (p31–43 and p58–89) was undertaken by parallel reaction monitoring (PRM) in positive ion mode. Chromatographic separation of peptides was performed as described in section 2.6. MS data were collected using: resolution, 30,000; AGC target, 1×10^5; maximum injection time, 50 ms; loop count, 5; isolation window, 0.8 *m/z*; normalized collision energy, 30 %. Accurate peptide quantification was achieved using an external calibration curve for each standard peptide in SPE eluate (matrix matched), at concentrations ranging from 10.0 to 1000 μg/mL. Extracted ion chromatograms were integrated using the Freestyle *v. 1.8* software from *Thermo Fisher Scientific* and peptide concentration determined by linear regression of the standard curve. The precursor ion *m/z* and quantifier fragment ions used during peptide quantification are detailed in Table 2.

2.9. Data analysis and processing

2.9.1. Bottom-up proteomics

Gluten protein identification and quantification was performed on the whole LFQ data set using the Proteome Discoverer (*v. 2.5.0.400*; *Thermo Fisher Scientific*, USA) search engine. The workflow used for data analysis was constituted by several processing and consensus steps including: (1) spectrum selector node: minimum precursor mass, 350 Da; maximum precursor mass, 5000 Da; retention time range, 0–70 min; S/N threshold (FT-only). 1.5; (2) Sequest HT node using a curated gluten protein database compiling 630 sequences (Bromilow et al., 2017);

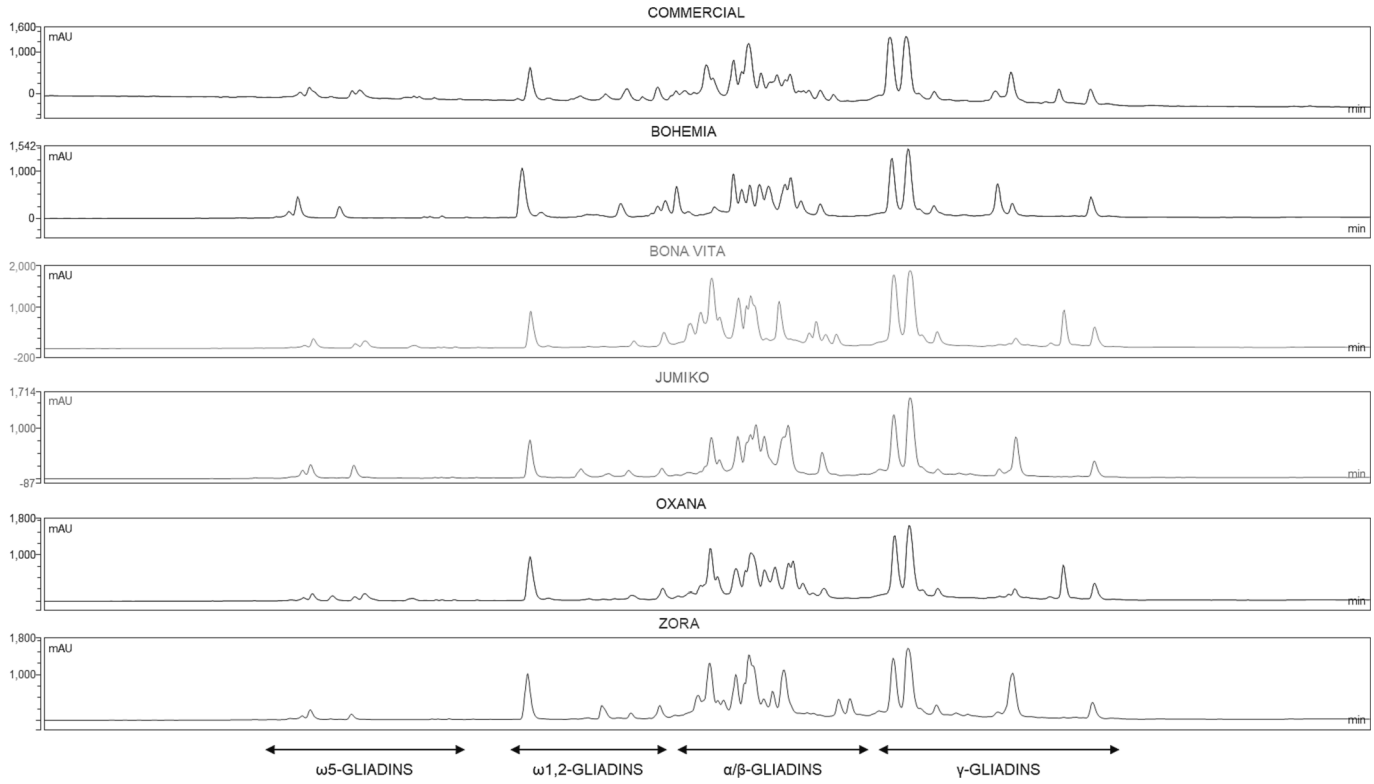

Fig. 1. HPLC profile of the six gliadin fractions isolated from pigmented and non-pigmented wheat flours. HPLC- high performance liquid chromatography.

enzyme, trypsin (semi); minimum peptide length, 5; maximum peptide length, 150; precursor mass tolerance, 10 ppm; fragment mass tolerance, 0.02 Da; dynamic modifications, oxidation (M), acetylation (N-terminus), M−loss, M−loss + acetylation; static modifications, cysteine carbamidomethylation; (3) percolator node: target/decoy selection, concatenated; validation based on q-value; maximum delta Cn, 0.05; target false discovery rate (FDR)(strict), 0.01; target FDR (relaxed), 0.05; (4) Minora node: minimum trace length, 5; S/N threshold, 1, maximum retention time difference of isotope pattern multiplets, 0.2 min; peptide-spectrum match (PSM) confidence of at least medium; (5) MSF file node: spectra to store, "identified or quantified", without merging identified peptides and proteins; (6) PSM grouper node using a site probability threshold of 75 %; (7) peptide validator node set to automatic (control peptide-level error rate if possible); (8) protein grouping applying a strict parsimony principle; (9) feature mapper node to perform a retention time alignment; coarse parameter tuning, maximum retention time shift, 5 min; retention time tolerance, 2 min; mass tolerance, 10 ppm; minimum S/N threshold, 5 min; (10) precursor ions quantifier node using "unique + razor" peptides; precursor abundance based on intensity; normalization mode using all peptides; protein abundance calculation given as the sum of the quantification values of all peptides belonging to that protein; N for Top N, 3; protein ration calculation based on pairwise ratio; maximum allowed fold change, 100; hypothesis test, *t*-test (background-based). Proteins not labelled as "*Is Master Protein*" were filtered out. The resulting data file can be consulted in Supplementary Material: "*Dataset 1 – Gliadin LFQ by DDA*".

Besides the content on CD-relevant T-cell epitopes (Sollid et al., 2020), the immunogenic potential of gluten proteins was complementarily accessed by using (1) RIDASCREEN gliadin assay (*R-Biopharm*, Germany) *i.e.* a R5 sandwich enzyme immunoassay based on specific monoclonal antibody to CD toxic sequences (QQPFP, QQQFP, LQPFP and QLPFP) to determine gliadin as a measure of gluten in food (Van Eckert et al., 2010) and (2) *preDQ* software tool from the *European Food Safety Authority* (EFSA) (Doytchinova, Dimitrov, & Atanasova, 2023). *preDQ* is a software utility that simulates deamidation and peptide binding to HLA-DQ2 (and HLA-DQ8) proteins and assesses the risk of CD induction by novel proteins. It employs five computational models based on datasets of known binding and non-binding peptides, using both ligand-based and structure-based *in silico* methods. These models are rigorously validated, and only the best-performing ones are included in *preDQ*, making it a reliable and user-friendly resource for evaluating peptide binding affinity and celiac disease risk associated with specific proteins (Doytchinova et al., 2023). The RIDASCREEN assay was performed in accordance with the manufacturer's instructions. Gliadin content was normalized to the total protein concentration, the latter quantified using the *Pierce BCA Protein Assay Kit* (*Thermo Fisher Scientific*, USA).

2.9.2. Gastrointestinal peptide profiling

Profiling of gluten digesta was performed as described in section 2.7.1. with some minor modifications: (1) no enzyme was specified; (2) dynamic modifications included oxidation (M) and pyroglutamination (Q); (3) PSM filter settings were defined to exclude peptides with confidence lower than "high", rank below 1, mass deviation (ppm) lower than −5 and higher than 5, and PSM ambiguity classified as "rejected". Only sequences identified in at least 2 technical replicates were further considered, keeping from those the highest recorded intensity value. The resulting data file can be consulted in Supplementary Material: "*Dataset 2 – INFOGEST peptide profiling*".

2.10. Statistical analysis

Targeted and untargeted composition analysis of at least three technical replicates were processed using Proteome Discoverer and GraphPad Prism v10 software for one-way ANOVA, unsupervised hierarchical clustering and principal component analysis (PCA). Hierarchical clustering was generated using complete linkage and Euclidean distance methods. When needed, hypothesis tests for comparing specific PSMs within different samples were conducted, using H_0: $\mu_1 - \mu_1 = 0$ and H_0: $\mu_1 - \mu_1 \neq 0$. The significance level was fixed at 5 % and the

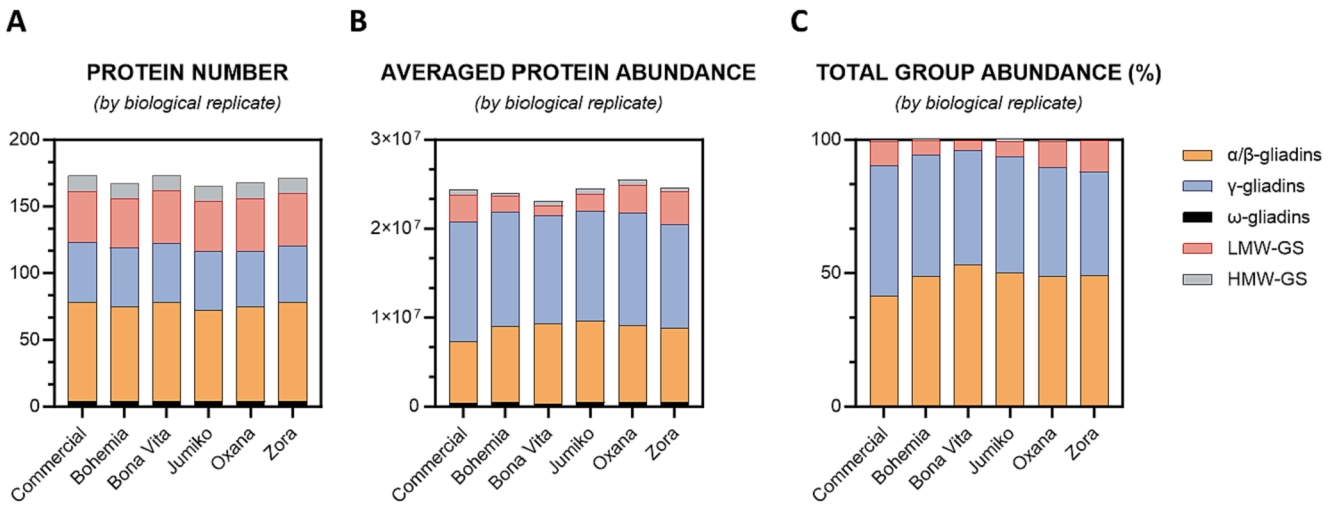

Fig. 2. Protein number (A), averaged protein abundance (B), and total group abundance (C), of gluten protein subtypes in each wheat-derived gliadin-rich extract.

distribution assumed to be two-tailed. Assuming two peptide groups – n_1 and n_2 – of equal variance (homoscedastic), but different standard deviations (s_1 and s_2), the pooled standard deviation (s_p) was calculated as follows (1):

$$s_p = \sqrt{\frac{(n_1 - 1)s_1^2 + (n_2 - 1)s_2^2}{n_1 + n_2 - 2}} \quad (1)$$

The test statistic was then calculated according to equation (2) were t^* follows a t-distribution with $n_1 + n_2 - 2$ degrees of freedom:

$$t^* = \frac{\overline{x}_1 - \overline{x}_2 - 0}{s_p\sqrt{\frac{1}{n_1} + \frac{1}{n_2}}} \quad (2)$$

where, $\overline{x}_1$ and $\overline{x}_2$ correspond to the sample average of group (1) and group (2), respectively.

3. Results and discussion

3.1. Gluten proteins profiling and quantification

The distribution of gliadin proteins into α/β-, γ-, ω1,2- and ω5-subtypes was first accessed by reversed-phase HPLC (Fig. 1) (Scherf, 2016). From this analysis, considerable differences were evidenced between samples regarding their protein expression fingerprint, particularly within the α/β- and γ-gliadin regions, as both areas showed almost unique distribution patterns. The proportion of gliadin subtypes, however, was very similar between varieties: [2.45–5.51] % for ω5-gliadins, [5.98–11.90] % for ω1,2-gliadins, [45.43–53.50] % for α/β-gliadins and [36.25–41.87] % for γ-gliadins (Fig. 1). The α/β:γ ratio, on the other hand, was around 1.1 and 1.4, the typical reported range for common wheat (Geisslitz, Wieser, Scherf, & Koehler, 2018; Pronin, Börner, Weber, & Scherf, 2020). In general, α/β-gliadins were the predominant type – particularly in the Bona Vita and Oxana varieties -, followed by γ-gliadins – found to be higher in the commercial flour. Altogether, this data suggests that regardless of these grain's having slightly different genetic backgrounds, their overall α/β-, γ-, ω1,2- and ω5-gliadin distribution is essentially the same.

To access the specific protein composition within each gliadin type and wheat variety, LFQ analyses were performed by mass spectrometry. Protein quantification, using the latest *Proteome Discoverer* bioinformatic tool, was based on both unique and razor peptides, followed by data normalization to the total peptide intensity (Palomba et al., 2021). According to Fig. 2, one may see that though α/β-gliadins occurrence was higher than that of γ-gliadins in terms of protein number and proportion (Fig. 2A, C), their averaged individual abundance was considerably lower than the latter (*p-value* = 0.057) (Fig. 2B). The overall trend, however, was quite similar to that observed by HPLC-based group integration, with the only exception that in this case a small percentage of co-extractable LMW- and HMW-GS were also identified. Interestingly, the contribution of LMW-GS to the total gliadin content in both Zora and Oxana varieties was significantly higher than that of the other whole-grain flours (Fig. 2C, *p-value* = 0.014), notwithstanding their lower sequence coverage (37 ± 10 % for LMW-GS *vs* 61 ± 10 % for α/β- and γ-gliadins, *p-value* < 0.001) and number of unique peptides quantified (68 for LMW-GS *vs* 315 for α/β- and γ-gliadins). Such outcome may, nevertheless, suggest differences in the intricacy of the gliadin-glutenin viscoelastic network in anthocyanin-rich wheat doughts, as already observed (Šebestíková, Burešová, Vyhnánek, Martinek, & Pospiech, 2023). Looking at the protein distribution within each gliadin class (Supplementary Figs. 1-3), one may observe a high degree of conservation in the gliadin expression profile between pigmented and non-pigmented wheat varieties – particularly amongst the most abundant ones. Quantitatively, however, the relative abundance of specific gliadin proteins varies considerably between samples (Table 3).

Table 3 summarizes the major changes observed in gliadins abundance between pigmented wheat varieties (grouped as one single dataset) relative to Bohemia (control strain). The commercial wheat sample was excluded from these analyses to avoid any source of variability (bias) introduced by its unknown origin, agronomic and environmental growth conditions and post-harvest processing. From the 24 most abundant α/β-gliadin proteins (summed contribution of 94.6 % to the total α/β-gliadin content), 14 of them revealed significant changes in their expression levels: 11 proteins were found downregulated in pigmented wheat flours while 3 others got upregulated, particularly in Bona Vita (*fold*-changes ranging from 2.3 to 7.1). Importantly, all downregulated α/β-gliadins were characterized by a strong immunogenic potential, as revealed by identification of CD-associated T-cell epitopes and the use of the *preDQ* software tool from EFSA (Doytchinova et al., 2023; Sollid et al., 2020). For γ-gliadins, 7 out of the 13 most abundant proteins were found downregulated, while for ω-gliadins only one (out of 4) had a significant negative change in its expression level. No upregulations were detected in both gliadin classes between pigmented and non-pigmented samples. These findings align with the outcomes of the RIDASCREEN assay, indicating a general decrease in gliadin immunoreactivity within pigmented wheat grains (Fig. 3). However, the detected levels still exceed the established regulatory threshold of 20 parts per million (ppm) considered as 'safe'.

Principal Component Analysis (PCA) using the aggregated abundance data for each genotype was additionally performed (Fig. 4).

Table 3
Gliadin proteins whose normalized abundance changed significantly within all pigmented *vs* non-pigmented wheat varieties (*i.e.* Bohemia). Only the most abundant proteins within each gliadin type were compared. The identification of CD-relevant T-cell epitopes were based on Sollid et al. (2020) and positive predictions [*i.e.* overall number of peptide sequences predicted to be HLA-DQ2.5 (A1*05:01/B1*02:01) binders] were obtained using the preDQ software tool from the European Food Safety Authority (EFSA).

Accession	Change	*p-value*	CD-relevant T-cell epitopes (α/β-gliadins)	Positive predictions
R9XUP7	↑	<0.001	DQ2.2-glia- α1	24
Q306G0	↓	<0.001	DQ2.5-glia- α1a, DQ2.5-glia-α3, DQ2.2-glia-α1, DQ2.2-glia-α2	26
Q9M4M1	↓	<0.001	DQ2.2-glia-α1, DQ2.2-glia-α2	21
I0IT59	↑	<0.001	—	26
Q9M4L9	↓	<0.001	DQ2.5-glia- α1a, DQ2.5-glia-α3, DQ2.2-glia-α1, DQ2.2-glia-α2	10
Q41530	↓	<0.001	DQ2.5-glia-α3, DQ2.2-glia-α1, DQ2.2-glia-α2	26
Q41545	↓	<0.001	DQ2.2-glia-α1	25
K7XE82	↓	0.049	DQ2.5-glia- α1a, DQ2.5-glia-α3, DQ2.2-glia-α1	27
A5JSA6	↓	<0.001	DQ2.5-glia-α1a, DQ2.5-glia-α1b, DQ2.5-glia-α2, DQ2.5-glia-α3, DQ2.2-glia-α1, DQ2.2-glia-α2, DQ8-glia-α1, DQ8.5-glia-α1	30
R9XW75	↓	<0.001	DQ2.2-glia-α1, DQ8-glia-α1, DQ8.5-glia-α1	26
B2ZRD1	↓	<0.001	DQ2.5-glia-α1a, DQ2.5-glia-α2, DQ2.5-glia-α3, DQ2.2-glia-α1, DQ2.2-glia-α2	28
I0IT62	↓	<0.001	DQ8-glia-α1, DQ8.5-glia-α1	29
K7XE90	↓	0.007	DQ2.5-glia-α1a, DQ2.5-glia-α1b, DQ2.5-glia-α2, DQ2.2-glia-α1, DQ2.2-glia-α2	26
X2KS61	↑	0.008	DQ2.5-glia-α1a, DQ2.5-glia-α2, DQ2.5-glia-α3, DQ2.2-glia-α1, DQ2.2-glia-α2, DQ8-glia-α1, DQ8.5-glia-α1	24
Accession	**Change**	***p-value***	**CD-relevant T-cell epitopes (γ-gliadins)**	**Positive predictions**
D0ES80	↓	0.04	DQ2.5-glia-γ1, DQ2.5-glia-γ2, DQ2.5-glia-γ4c, DQ2.5-glia-γ4d, DQ8-glia-γ1a, DQ8-glia-γ2, DQ8.5-glia-γ1	29
B6UKP2	↓	0.006	DQ2.5-glia-γ1, DQ2.5-glia-γ2, DQ2.5-glia-γ3, DQ2.5-glia-γ4c, DQ8-glia-γ1a, DQ8-glia-γ1b, DQ8-glia-γ2, DQ8.5-glia-γ1	22
B6UKM5	↓	0.02	DQ2.5-glia-γ1, DQ2.5-glia-γ2, DQ2.5-glia-γ4b, DQ2.5-glia-γ4c, DQ8-glia-γ1a, DQ8-glia-γ2, DQ8.5-glia-γ1	31
D0ES81	↓	0.04	DQ2.5-glia-γ1, DQ2.5-glia-γ2, DQ2.5-glia-γ4b, DQ2.5-glia-γ4c, DQ2.5-glia-ω1, DQ2.5-hor-1, DQ2.5-*sec*-1, DQ8-glia-γ1a, DQ8-glia-γ2, DQ8.5-glia-γ1	32
R9XT02	↓	<0.001	DQ2.5-glia-γ1, DQ2.5-glia-γ2, DQ2.5-glia-γ4c, DQ2.5-glia-γ4e, DQ2.5-glia-γ5, DQ8-glia-γ1a, DQ8-glia-γ2, DQ8.5-glia-γ1	37
Q94G97	↓	<0.001	DQ2.5-glia-γ2, DQ2.5-glia-γ4c, DQ8-glia-γ1a	25
B6UKN7	↓	0.04	DQ2.5-glia-γ2, DQ2.5-glia-γ4c, DQ2.5-glia-γ4d, DQ2.5-glia-ω1, DQ2.5-hor-1, DQ2.5-*sec*-1, DQ8-glia-γ1a	32

Table 3 (*continued*)

Accession	Change	*p-value*	CD-relevant T-cell epitopes (α/β-gliadins)	Positive predictions
Accession	**Change**	***p-value***	**CD-relevant T-cell epitopes (ϖ-gliadins)**	**Positive predictions**
Q402I5	↓	<0.001	—	120

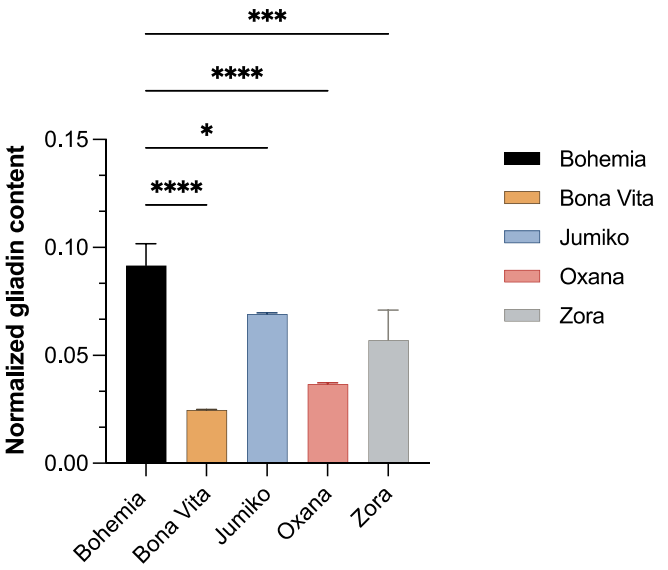

Fig. 3. Normalized gliadin content in wholegrain wheat flours as determined by the RIDASCREEN assay (expressed in mg of gliadins per mg of hydro-alcoholic extract). Bars represent mean values ± standard deviation. *p < 0.05, ***p < 0.001, ****p < 0.001.

Though not very informative, as PC1 and PC2 accounted for only 43 % of variation, one can still recognize a cluster made of Jumiko, Oxana and Zora varieties, whose dispersion along PC1 and PC2 closely relates them. Such trend is notably intriguing, as all three varieties exhibit high anthocyanin content in their grains, a factor that could potentially elucidate the similarity in their gliadin expression patterns. This suggests a potential correlation between anthocyanin accumulation and gliadin downregulation at the grain level, though differences in their genetic background prevents us from stating this unequivocally (Table 1). The Bona Vita sample, on the other hand, as a carotenoid-rich variety, has less variability over PC2 than PC1, making her distinguishably more like Jumiko, Oxana and Zora varieties than Bohemia. As for the commercial flour, though included, it does not have any special representativity in such comparisons, notwithstanding its closer resemblance to the pigmented wheat varieties than Bohemia itself.

Altogether, this data suggests that current breading programs aiming at increasing the concentration levels of specific bioactive compounds in the aleurone or pericarp layer of wheat grains might significantly impact the expression pattern and potential immunogenicity of gliadin proteins.

3.2. *Assessment of gliadin digestibility and release of bioactive peptides*

The standardized INFOGEST approach has been used to enzymatically digest the gliadin preparation obtained from both pigmented and non-pigmented wholegrain flours, with the aim of identifying and comparing the gliadin peptides that are likely to be physiologically released within the intestinal lumen. As it might be seen in Fig. 5A, no statistically significant differences were observed in peptide size distribution (MH^+) between samples, except for Zora, whose averaged molecular weight was slightly higher than that of Bohemia (*p-value* =

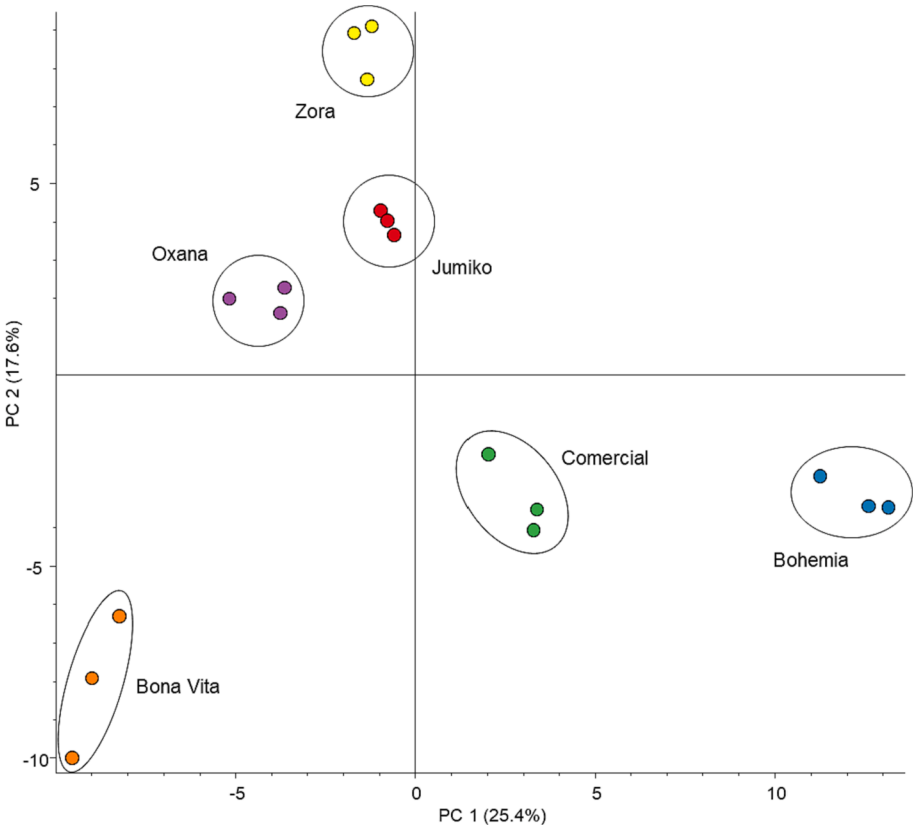

Fig. 4. Principal component analysis (PCA) based on the normalized abundance of gluten proteins per wheat grain/flour variety. No substantial variability in the distribution of protein abundance between technical replicates was detected.

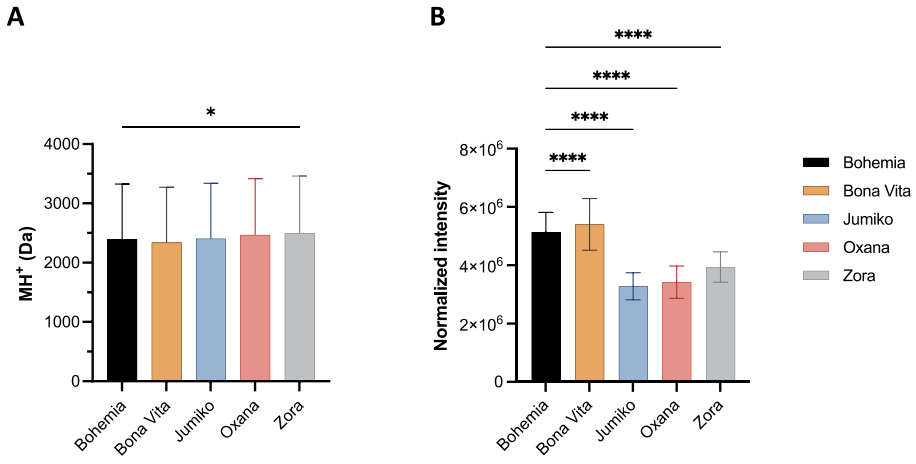

Fig. 5. Molecular weight distribution of gluten peptides (A) and normalized XIC intensities for sequences containing at least one of the following CD-relevant T-cell epitopes: PFPQPQLPY (DQ2.5-glia-α1a), PYPQPQLPY (DQ2.5-glia-α1b), PQPQLPYPQ (DQ2.5-glia-α2), FRPQQPYPQ (DQ2.5-glia-α3), PQQSFPQQQ (DQ2.5-glia-γ1), IQPQQPAQL (DQ2.5-glia-γ2), QQPQQPYPQ (DQ2.5-glia-γ3), SQPQQQFPQ (DQ2.5-glia-γ4a), PQPQQQFPQ (DQ2.5-glia-γ4b), QQPQQPFPQ (DQ2.5-glia-γ4c), PQPQQPFCQ (DQ2.5-glia-γ4d), LQPQQPFPQ (DQ2.5-glia-γ4e), QQPFPQQPQ (DQ2.5-glia-γ5), PFPQPQQPF (DQ2.5-glia-ω1), PQPQQPFPW (DQ2.5-glia-ω2), PFSQQQQPV (DQ2.5-glut-L1), FSQQQQSPF (DQ2.5-glut-L2), PFPQPQQPF (DQ2.5-hor-1), PQPQQPFPQ (DQ2.5-hor-2), PIPQQPQPY (DQ2.5-hor-3a), PYPQQPQPY (DQ2.5-hor-3b), PFPQPQQPF (DQ2.5-*sec*-1), DQ2.5-*sec*-2 (PQPQQPFPQ), PFPQQPEQI (DQ2.5-*sec*-3) PYPEQQEPF (DQ2.5-ave-1a), PYPEQQQPF (DQ2.5-ave-1b), PYPEQQQPI (DQ2.5-ave-1c), PFSQQQQPV (DQ2.2-glut-L1), QGSVQPQQL (DQ2.2-glia-α1), QYSQPQQPI (DQ2.2-glia-α2), QGSFQPSQQ (DQ8-glia-α1), QQPQQPFPQ (DQ8-glia-γ1a), QQPQQPYPQ (DQ8-glia-γ1b), PQQSFPQQQ (DQ8-glia-γ2), QGYYPTSPQ (DQ8-glut-H1), QGSFQPSQQ (DQ8.5-glia-α1), PQQSFPQQQ (DQ8.5-glia-γ1), QGYYPTSPQ (DQ8.5-glut-H1). Bars represent mean values ± standard deviation. *p < 0.05, ****p < 0.0001. Ion intensities have been normalized for the peptide load.

0.037).

Overall, 2438 different PSM's were identified: 1198 in Bohemia, 1042 in Bona Vita, 961 in Jumiko, 1055 in Oxana and 1118 in Zora. From those, 1039 contained at least one of the following immunoreactive peptide sequences: PFPQPQLPY (DQ2.5-glia-α1a), PYPQPQLPY (DQ2.5-glia-α1b), PQPQLPYPQ (DQ2.5-glia-α2), FRPQQPYPQ (DQ2.5-glia-α3), PQQSFPQQQ (DQ2.5-glia-γ1), IQPQQPAQL (DQ2.5-glia-γ2), QQPQQPYPQ (DQ2.5-glia-γ3), SQPQQQFPQ

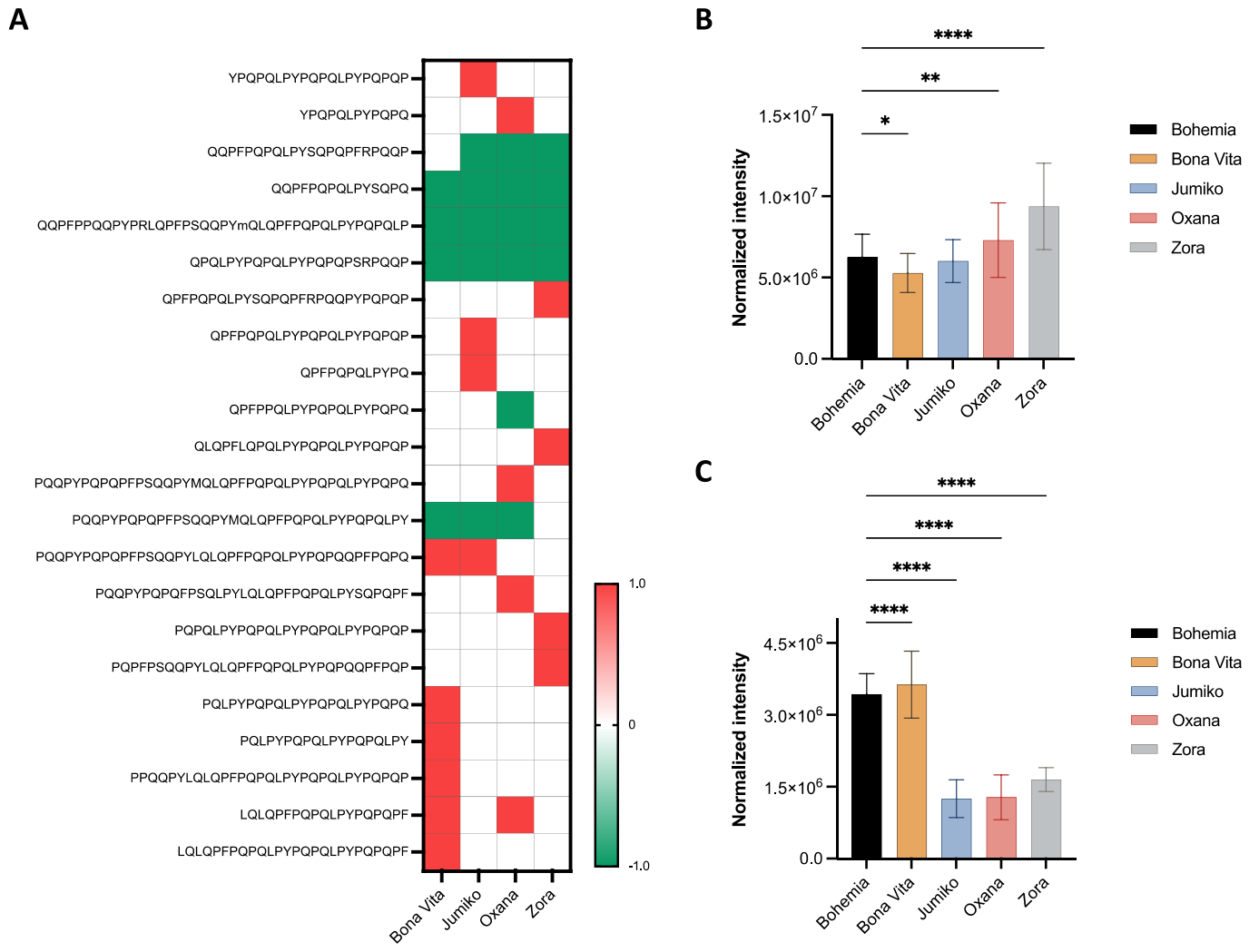

Fig. 6. Heatmap analysis (A) and normalized XIC intensities (B) of peptides containing at least one copy of PFPQPQLPY (DQ2.5-glia-α1a), PYPQPQLPY (DQ2.5-glia-α1b) or PQPQLPYPQ (DQ2.5-glia-α2) T-cell epitopes in pigmented wheat grains. Only sequences showing statistically different changes to Bohemia are shown in (A) ($p < 0.05$). Red colour means "overproduction" while green colour means "underproduction" or absence. (C) Normalized XIC intensities of peptides containing at least one copy of DQ2.5-glia-$\gamma_{1\text{-}5}$ T-cell epitopes. Bars represent mean values ± standard deviation. *$p < 0.05$, **$p < 0.01$, ****$p < 0.0001$. Ion intensities have been normalized for the peptide load. (For interpretation of the references to color in this figure legend, the reader is referred to the web version of this article.)

(DQ2.5-glia-γ4a), PQPQQQFPQ (DQ2.5-glia-γ4b), QQPQQPFPQ (DQ2.5-glia-γ4c), PQPQQPFCQ (DQ2.5-glia-γ4d), LQPQQPFPQ (DQ2.5-glia-γ4e), QQPFPQQPQ (DQ2.5-glia-γ5), PFPQPQQPF (DQ2.5-glia-ω1), PQPQQPFPW (DQ2.5-glia-ω2), PFSQQQQPV (DQ2.5-glut-L1), FSQQQQSPF (DQ2.5-glut-L2), PFPQPQQPF (DQ2.5-hor-1), PQPQQPFPQ (DQ2.5-hor-2), PIPQQPQPY (DQ2.5-hor-3a), PYPQQPQPY (DQ2.5-hor-3b), PFPQPQQPF (DQ2.5-*sec*-1), DQ2.5-*sec*-2 (PQPQQPFPQ), PFPQQPEQI (DQ2.5-*sec*-3) PYPEQQEPF (DQ2.5-ave-1a), PYPEQQQPF (DQ2.5-ave-1b), PYPEQQQPI (DQ2.5-ave-1c), PFSQQQQPV (DQ2.2-glut-L1), QGSVQPQQL (DQ2.2-glia-α1), QYSQPQQPI (DQ2.2-glia-α2), QGSFQPSQQ (DQ8-glia-α1), QQPQQPFPQ (DQ8-glia-γ1a), QQPQQPYPQ (DQ8-glia-γ1b), PQQSFPQQQ (DQ8-glia-γ2), QGYYPTSPQ (DQ8-glut-H1), QGSFQPSQQ (DQ8.5-glia-α1), PQQSFPQQQ (DQ8.5-glia-γ1), QGYYPTSPQ (DQ8.5-glut-H1) (Sollid et al., 2020). The distribution of these PSMs was roughly consistent across the various wheat varieties, with the following counts: 494 PSMs in Bohemia (41.2 %), 412 in Bona Vita (39.5 %), 425 in Jumiko (44.2 %), 449 in Oxana (42.6 %), and 517 in Zora (46.2 %). However, the representativeness of these PSMs within each sample (measured as the peak height at the apex of the chromatographic profile) differed significantly (Fig. 5B). Notably, Zora, Oxana, and Jumiko's gliadin digestion led to substantially lower levels of immunogenic peptide sequences released during both gastric and pancreatic processing when compared to Bohemia, and most important, to Bona Vita's digestion. Among all the wheat varieties examined, Bona Vita exhibited the most pronounced accumulation of immunoreactive peptide sequences, notwithstanding its lower response towards the R5-mAb (Fig. 3). This phenomenon suggests sort of a genotype-dependency, which could be linked to variations in both the abundance and specific distribution of immunogenic gliadin proteins that cannot be accurately accounted by the RIDASCREEN assay (recognizing epitopes with the amino acid sequence QQPFP the greatest). For instance, when analysing the proteins that exhibited a differential expression between Bona Vita and the cluster of anthocyanin-rich grains (Fig. 4), a total of 17 α/β-gliadins displayed considerable changes, with 13 of them trending towards higher concentrations ($p < 0.05$): K7WV37, R9XUP7, J7I026, I0IT51, R9XUN7, X2KVH9, R9XSU5, K7XE64, J7HT18, I0IT63, I0IT60, I0IT55, I0IT52 (Supplementary Fig. 1). Each of the latter 13 proteins contained at least one copy of the following immunostimulatory T-cell epitopes: DQ2.5-glia-α1a, DQ2.5-glia-α1b, DQ2.5-glia-α2, DQ2.5-glia-α3, DQ2.2-glia-α1, DQ2.2-glia-α2, DQ8-glia-α1 and/or DQ8.5-glia-α1. Similar discrepancies were also found within the γ-gliadin subgroup, including for the Q6EEX1, K7X0M3, B6DQB8,B6UKP1, Q9M4M4, B6UKN9, K7XE64, X2KWL1, R4VEK6, R9XV20, Q94G97, R9XUQ5,

Table 4
Quantification of p58–89, and p31–43 content (expressed in μg of peptide per milligram of dry weight) in pigmented and non-pigmented gliadin digestions. Data is presented as mean values ± standard deviation.

Wheat variety	Overall peptide content[1] (μg/mg digesta)	P58–89[2] (μg/mg digesta)	P31–43[3] (μg/mg of digesta)
Bohemia	400 ± 7	0.0082 ± 0.0007[4]	0.10 ± 0.02
Bona Vita	450 ± 9	0.0556 ± 0.0008[4]	0.029 ± 0.006[5]
AF Jumiko	438 ± 7	0.024 ± 0.001[4]	0.06 ± 0.01
AF Oxana	458 ± 15	0.0105 ± 0.0007[4]	0.04 ± 0.01[5]
AF Zora	451 ± 5	0.0069 ± 0.0006[4]	0.041 ± 0.007[5]

[1] Determined using the Pierce™ quantitative peptide assay (Thermo Fisher Scientific).
[2] Linear correlation: XIC area = $1.24 \times 10^9 \times$ [p58–89] (0.01–1.0 μg/mL), $R^2 = 0.9919$, LOD = 0.16 μg/mL, LOQ = 0.47 μg/mL.
[3] Linear correlation: XIC area = $1.57 \times 10^9 \times$ [p31–43] (0.001–0.5 μg/mL), $R^2 = 0.9967$, LOD = 0.02 μg/mL, LOQ = 0.06 μg/mL.
[4] Calculated from value below the theoretical LOD and LOQ.
[5] Calculated from value below the theoretical LOQ.

K7X1J5, K7WVB5, and R9XSZ2 proteins, whose abundance is shown to be significantly higher in Bona Vita's grains (Supplementary Fig. 2). The contrasting responses of gliadin protein expression – and dynamic behaviour during gastrointestinal processing – in carotenoid-rich grains compared to anthocyanin-rich grains might thus be a contributing factor to the elevated immunogenic potential of Bona Vita-derived peptides (Perez-Gregorio, Dias, Mateus, & De Freitas, 2018).

Of note, and notwithstanding the statistical significance of Figure's 5 dataset, some contextual factors, research methodology, and potential sources of bias must be accounted for when categorizing the immunogenicity of gliadin digestions. As no T-cell assays were performed at this point, adherence to these precautions is crucial to enhance the robustness and reliability of assessments regarding the immunogenic potential of gliadin digestions. First, it has been assumed that all immunoreactive peptide sequences identified herein can trigger a gliadin-specific T-cell response of the same magnitude and dose relationship. That's actually not the case, as intestinal T-cell responses to gluten peptides are now known to be largely heterogeneous, hierarchical and deamidation-dependent (Camarca et al., 2009). Also, the distribution and abundance of peptides harboring T-cell nonamers exhibit a grain-specific pattern, as depicted in Fig. 6 for the gliadin epitopes DQ2.5-glia-α1a, DQ2.5-glia-α1b, DQ2.5-glia-α2, and DQ2.5-glia-γ1-5. Their release, in comparison to Bohemia, was observed to be differentially regulated, and predominantly contrasting in sequences containing DQ2.5-glia-γ4a-e epitopes (*data not shown*).

Secondly, it has been assumed that the intensity of ion current measured by the mass spectrometer represents an accurate estimation of relative peptide abundance between samples. This, however, may not be true if one accounts for charge competition or ionization inefficiency effects in complex matrices, leading, as consequence, to differences in the linear dynamic range and detection limit of the same analyte. To check this, PRM-targeted experiments on gastrointestinal digests were conducted to quantify the levels of two distinct immunostimulatory peptides within each gliadin digestion: p58–89 and p31–43 (Table 4). p58–89 (*i.e.* 33-mer peptide without the initial leucine residue) was nearly detectable (*i.e.* < LOD) in its intact form by both targeted and untargeted approaches. p31–43, on the other hand, was found to be present at a significantly higher concentration in Bohemia's samples ($p < 0.0001$), and at lower concentration in those from Bona Vita. A similar trend was also observed by monitoring changes on p31–43 peptide intensity by untargeted DDA (Supplementary Fig. 4), which, though intrinsically stochastic, provided a reliable measurement of gluten peptides' abundance (and protein concentration).

Importantly, gliadin p31–43 does not bind to HLA class II molecules or induce T-cell activation as p58–89 does (Calvanese et al., 2019). On the contrary, it acts as an inducer of multiple pro-inflammatory and toxic effects *in vivo*, including the upregulation of NLRP3 inflammasome/caspase 1-dependent mucosal damage of the small intestine (Gómez Castro et al., 2019). As a representative of "innate" immunity, the upregulation of p31–43 levels in Bohemia's digestion (non-pigmented control grain) strengthens its category as – in theory – the most toxic variety of the ones tested herein, only comparable with Bona Vita's in terms of immunogenic peptides abundance (Fig. 5B).

4. Conclusion

Over the past few years, many efforts have placed on the development of biofortified coloured wheat varieties with enhanced nutritional, agronomical, technological and functional health benefits. While phenolics and related compounds have been a primary focus, recent exploration has revealed substantial improvements in both protein content and amino acid profiles (Tian, Chen, & Wei, 2018). Nevertheless, the distribution, digestibility, and immunogenicity of specific gluten proteins – the main environmental triggers of CD -, have remained largely uncharted. Herein, we provide a comprehensive proteomic-based assessment on the immunogenicity of gliadin proteins and peptides from novel anthocyanin- and carotenoid-rich wheat varieties by (semi)-quantitative high resolution mass spectrometry. It has been found that gliadin expression and peptide release following a simulated gastrointestinal digestion – particularly those containing CD-immunostimulatory γ-gliadin epitopes – is differential and grain-dependent, and that anthocyanin accumulation, as opposed to carotenoids, correlated with a lower immunogenicity and toxicity of gliadins at both protein and peptide levels. Considering that the amount of immunogenic peptides is the primary factor necessary for the achievement of the threshold for the inflammatory response mediated by T-cells in subjects genetically predisposed to have CD, the consumption of pigmented cereals with a reduced load of gluten epitopes, could be a way to maintain the pathogenic T-cells below the threshold of the inflammatory cascade, thus preventing, or delaying, the detrimental autoimmune response in genetically at-risk individuals (Aronsson et al., 2016; Størdal, White, & Eggesbø, 2013). This, however, has yet to be corroborated with further studies, that might include, for instance, *ex-vivo* experiments and/or *in vivo* T-cell assays (Gianfrani et al., 2015; Picascia et al., 2020). It also is essential, within each wheat sample, to subject more intricate matrices to testing to understand how these naturally present anthocyanin and carotenoid compound impact gliadin catabolism, as well as the bioavailability and bioactivity of immunogenic peptides throughout the gastrointestinal tract.

Funding

This work was financially supported through the project UIDB/50006/2020, funded by FCT/MCTES through national funds, and by The European Food Risk Assessment Fellowship Programme (GP/EFSA/ENREL/2022/02).

CRediT authorship contribution statement

Ricardo Dias: Conceptualization, Methodology, Supervision, Writing – original draft, Funding acquisition. **Sara da Silva:** Investigation. **Bruna Monteiro:** Investigation. **Rosa Pérez-Gregorio:** Writing – original draft, Investigation. **Nuno Mateus:** Funding acquisition, Project administration, Writing – review & editing. **Carmen Gianfrani:** Writing – review & editing. **Maria Vittoria Barone:** Writing – review & editing. **Petr Martinek:** Investigation, Resources, Writing – review & editing. **Victor Freitas:** Funding acquisition, Project administration, Writing –

review & editing.

Declaration of competing interest

The authors declare that they have no known competing financial interests or personal relationships that could have appeared to influence the work reported in this paper.

Data availability

Proteomic data is now available on ProteomeXchange

Acknowledgements

The authors would like to acknowledge FCT (Foundation for Science and Technology) for the Scientific Employment Stimulus grant (*2021.01830.CEECIND*). *PM* also thanks to the project QL24010230 of the Ministry of Agriculture of the Czech Republic. *RPG* would like to thank the Ramón y Cajal contract RYC2021-033224-I, funded by the Spanish Ministry of Science and Innovation and the National Agency for Research (0000421S140.06) from the Spain Govern (MCIN/AEI/10.13039/501100011033) and the European Union under the frame of "NextGenerationEU/PRTR" funds.

Appendix A. Supplementary data

Supplementary data to this article can be found online at https://doi.org/10.1016/j.foodres.2024.114008.

References

Abdel-Aal, E.-S.-M., Abou-Arab, A. A., Gamel, T. H., Hucl, P., Young, J. C., & Rabalski, I. (2008). Fractionation of blue wheat anthocyanin compounds and their contribution to antioxidant properties. *Journal of Agricultural and Food Chemistry, 56*(23), 11171–11177.

Abdel-Aal, E.-S.-M., Hucl, P., Shipp, J., & Rabalski, I. (2016). Compositional differences in anthocyanins from blue- and purple-grained spring wheat grown in four environments in central Saskatchewan. *Cereal Chemistry, 93*(1), 32–38.

Aronsson, C. A., Lee, H.-S., Koletzko, S., Uusitalo, U., Yang, J., Virtanen, S. M., … Agardh, D. (2016). Effects of gluten intake on risk of celiac disease: A case-control study on a Swedish birth cohort. *Clinical Gastroenterology and Hepatology, 14*(3), 403-409. e403.

Awika, J. M. (2011). Major Cereal Grains Production and Use around the World. In *Advances in Cereal Science: Implications to Food Processing and Health Promotion* (Vol. 1089, pp. 1–13). American Chemical Society.

Brodkorb, A., Egger, L., Alminger, M., Alvito, P., Assunção, R., Ballance, S., … Carrière, F. (2019). INFOGEST static in vitro simulation of gastrointestinal food digestion. *Nature Protocols, 14*(4), 991–1014.

Bromilow, S., Gethings, L. A., Buckley, M., Bromley, M., Shewry, P. R., Langridge, J. I., & Mills, E. C. (2017). A curated gluten protein sequence database to support development of proteomics methods for determination of gluten in gluten-free foods. *Journal of Proteomics, 163*, 67–75.

Calvanese, L., Nanayakkara, M., Aitoro, R., Sanseverino, M., Tornesello, A. L., Falcigno, L., … Barone, M. V. (2019). Structural insights on P31–43, a gliadin peptide able to promote an innate but not an adaptive response in celiac disease. *Journal of Peptide Science, 25*(5), e3161.

Camarca, A., Anderson, R. P., Mamone, G., Fierro, O., Facchiano, A., Costantini, S., … Sette, A. (2009). Intestinal T cell responses to gluten peptides are largely heterogeneous: Implications for a peptide-based therapy in celiac disease. *The Journal of Immunology, 182*(7), 4158–4166.

Cappelli, A., & Cini, E. (2021). Challenges and opportunities in wheat flour, pasta, bread, and bakery product production chains: A systematic review of innovations and improvement strategies to increase sustainability, productivity, and product quality. *Sustainability, 13*(5), 2608.

da Silva, S., Pérez-Gregorio, R., Mateus, N., Freitas, V., & Dias, R. (2023). Evidence of increased gluten-induced perturbations in the nucleophilic tone and detoxifying defences of intestinal epithelial cells impaired by gastric disfunction. *Food Research International, 173*, Article 113317.

Dias, R., Pereira, C. B., Pérez-Gregorio, R., Mateus, N., & Freitas, V. (2021). Recent advances on dietary polyphenol's potential roles in Celiac Disease. *Trends in Food Science & Technology, 107*, 213–225.

Doytchinova, I., Dimitrov, I., & Atanasova, M. (2023). preDQ–a software tool for peptide binding prediction to HLA-DQ2 and HLA-DQ8. *EFSA Supporting Publications, 20*(7), 8108E.

Erenstein, O., Jaleta, M., Mottaleb, K. A., Sonder, K., Donovan, J., & Braun, H.-J. (2022). Global trends in wheat production, consumption and trade. In M. P. Reynolds, & H.-J. Braun (Eds.), *Wheat improvement: Food security in a changing climate* (pp. 47–66). Cham: Springer International Publishing.

Ficco, D. B. M., De Simone, V., Colecchia, S. A., Pecorella, I., Platani, C., Nigro, F., Finocchiaro, F., Papa, R., & De Vita, P. (2014). Genetic Variability in Anthocyanin Composition and Nutritional Properties of Blue, Purple, and Red Bread (Triticum aestivum L.) and Durum (Triticum turgidum L. ssp. turgidum convar. durum) Wheats. *Journal of Agricultural and Food Chemistry, 62* (34), 8686-8695.

Garg, M., Kaur, S., Sharma, A., Kumari, A., Tiwari, V., Sharma, S., … Krishania, M. (2022). Rising demand for healthy foods-anthocyanin biofortified colored wheat is a new research trend. *Frontiers Nutrition, 9*.

Geisslitz, S., Wieser, H., Scherf, K. A., & Koehler, P. (2018). Gluten protein composition and aggregation properties as predictors for bread volume of common wheat, spelt, durum wheat, emmer and einkorn. *Journal of Cereal Science, 83*, 204–212.

Gianfrani, C., Camarca, A., Mazzarella, G., Di Stasio, L., Giardullo, N., Ferranti, P., … Troncone, R. (2015). Extensive in vitro gastrointestinal digestion markedly reduces the immune-toxicity of Triticum monococcum wheat: Implication for celiac disease. *Molecular Nutrition & Food Research, 59*(9), 1844–1854.

Gómez Castro, M. F., Miculán, E., Herrera, M. G., Ruera, C., Perez, F., Prieto, E. D., … Chirdo, F. G. (2019). P31–43 gliadin peptide forms oligomers and induces NLRP3 inflammasome/caspase 1-dependent mucosal damage in small intestine. *Frontiers in Immunology, 10*, 31.

Gozzi, M., Blandino, M., Dall'Asta, C., Martinek, P., Bruni, R., & Righetti, L. (2023). Anthocyanin Content and Fusarium Mycotoxins in Pigmented Wheat (Triticum aestivum L. spp. aestivum): An Open Field Evaluation. *Plants, 12* (4), 693.

Lachman, J., Martinek, P., Kotíková, Z., Orsák, M., & Šulc, M. (2017). Genetics and chemistry of pigments in wheat grain – A review. *Journal of Cereal Science, 74*, 145–154.

Palomba, A., Abbondio, M., Fiorito, G., Uzzau, S., Pagnozzi, D., & Tanca, A. (2021). Comparative evaluation of MaxQuant and proteome discoverer MS1-based protein quantification tools. *Journal of proteome research, 20*(7), 3497–3507.

Paznocht, L., Burešová, B., Kotíková, Z., & Martinek, P. (2021). Carotenoid content of extruded and puffed products made of colored-grain wheats. *Food Chemistry, 340*, Article 127951.

Perez-Gregorio, M., Dias, R., Mateus, N., & De Freitas, V. (2018). Identification and characterization of proteolytically resistant gluten-derived peptides. *Food & function, 9*(3), 1726–1735.

Picascia, S., Camarca, A., Malamisura, M., Mandile, R., Galatola, M., Cielo, D., … Troncone, R. (2020). In celiac disease patients the in vivo challenge with the diploid Triticum monococcum elicits a reduced immune response compared to hexaploid wheat. *Molecular Nutrition & Food Research, 64*(11), 1901032.

Pronin, D., Börner, A., Weber, H., & Scherf, K. A. (2020). Wheat (Triticum aestivum L.) breeding from 1891 to 2010 contributed to increasing yield and glutenin contents but decreasing protein and gliadin contents. *Journal of Agricultural and Food Chemistry, 68*(46), 13247–13256.

Reynolds, A. N., Akerman, A. P., & Mann, J. (2020). Dietary fibre and whole grains in diabetes management: Systematic review and meta-analyses. *PLoS Medicine, 17*(3), e1003053.

Ribeiro, M., Sousa, T. d., Poeta, P., Bagulho, A. S., & Igrejas, G. (2020). Review of structural features and binding capacity of polyphenols to gluten proteins and peptides in vitro: Relevance to celiac disease. *Antioxidants, 9* (6), 463.

Saini, P., Kumar, N., Kumar, S., Mwaurah, P. W., Panghal, A., Attkan, A. K., … Singh, V. (2021). Bioactive compounds, nutritional benefits and food applications of colored wheat: A comprehensive review. *Critical Reviews in Food Science and Nutrition, 61* (19), 3197–3210.

Sardella, C., Burešová, B., Kotíková, Z., Martinek, P., Meloni, R., Paznocht, L., … Blandino, M. (2023). Influence of Agronomic Practices on the Antioxidant Compounds of Pigmented Wheat (Triticum aestivum spp. aestivum L.) and Tritordeum (× Tritordeum martinii A. Pujadas, nothosp. nov.) Genotypes. *Journal of Agricultural and Food Chemistry, 71*(36), 13220–13233.

Scherf, K. A. (2016). Impact of the preparation procedure on gliadin, glutenin and gluten contents of wheat starches determined by RP-HPLC and ELISA. *European Food Research and Technology, 242*(11), 1837–1848.

Šebestíková, R., Burešová, I., Vyhnánek, T., Martinek, P., & Pospiech, M. (2023). Rheological and fermentation properties of doughs and quality of breads from colored wheat varieties. *Heliyon, 9*(4).

Sollid, L. M., Tye-Din, J. A., Qiao, S. W., Anderson, R. P., Gianfrani, C., & Koning, F. (2020). Update 2020: Nomenclature and listing of celiac disease-relevant gluten epitopes recognized by CD4(+) T cells. *Immunogenetics, 72*(1–2), 85–88.

Størdal, K., White, R. A., & Eggesbø, M. (2013). Early feeding and risk of celiac disease in a prospective birth cohort. *Pediatrics, 132*(5), e1202–e1209.

Tian, S.-Q., Chen, Z.-C., & Wei, Y.-C. (2018). Measurement of colour-grained wheat nutrient compounds and the application of combination technology in dough. *Journal of Cereal Science, 83*, 63–67.

Van Eckert, R., Bond, J., Rawson, P., Klein, C. L., Stern, M., & Jordan, T. (2010). Reactivity of gluten detecting monoclonal antibodies to a gliadin reference material. *Journal of Cereal Science, 51*(2), 198–204.

Zhang, B., Zhao, Q., Guo, W., Bao, W., & Wang, X. (2018). Association of whole grain intake with all-cause, cardiovascular, and cancer mortality: A systematic review and dose-response meta-analysis from prospective cohort studies. *European Journal of Clinical Nutrition, 72*(1), 57–65.